Inorg. Chem. **2008**, *47*, 4146−4152

ZnO Twin-Cones: Synthesis, Photoluminescence, and Catalytic Decomposition of Ammonium Perchlorate

Xuefei Sun, Xiaoqing Qiu, Liping Li, and Guangshe Li*

State Key Laboratory of Structural Chemistry, Fujian Institute of Research on the Structure of Matter, and Graduate School of Chinese Academy of Sciences, Fuzhou 350002, People's Republic of China

Received October 10, 2007

ZnO twin-cones, a new member to the ZnO family, were prepared directly by a solvothermal method using a mixed solution of zinc nitrate and ethanol. The reaction and growth mechanisms of ZnO twin-cones were investigated by X-ray diffraction, UV–visible spectra, infrared and ion trap mass spectra, and transmission electron microscopy. All as-prepared ZnO cones consisted of tiny single crystals with lengths of several micrometers. With prolonging of the reaction time from 1.5 h to 7 days, the twin-cone shape did not change at all, while the lattice parameters increased slightly and the emission peak of photoluminescence shifted from the green region to the near orange region. ZnO twin-cones are also explored as an additive to promote the thermal decomposition of ammonium perchlorate. The variations of photoluminescence spectra and catalytic roles in ammonium perchlorate decomposition were discussed in terms of the defect structure of ZnO twin-cones.

1. Introduction

ZnO belongs to a kind of wide band gap semiconductors that have huge potential applications for light-emitting diodes, field-effect transistors, ultraviolet lasers, catalysis, gas sensors, solar cells, and diluted magnetic semiconductors.[1–3] As for many other semiconductors, the physical properties of ZnO are determined by particle shape and sample uniformity. Extensive physical and chemical approaches have been employed to synthesize various crystalline shapes of ZnO[4–9] with an aim to tailor the properties for advanced technological uses. Physical methods[5–7] have yielded ZnO tubes, springs, and comblike shapes, which however show disadvantages of requiring either extreme conditions or expensive equipments. Wet chemical syntheses have recently become the priority that one has frequently taken to explore the distinct morphologies. Nevertheless, to achieve low-temperature synthesis, majority of the previous wet chemical routes have to adopt various bases including NaOH, LiOH, or KOH[10] to promote the hydrolysis of zinc salts in water or alcohols. Even in the case when a very low concentration of strong bases was involved in the reactions, some amounts of exotic metal ions may incorporate in ZnO lattice, creating unintentional defect levels and moreover putting serious damages on the material properties.[11]

Templates including surfactants and polymers have been used as the additives to assist in retaining the special morphology of ZnO products.[12–14] However, addition of surfactants or polymers to the reaction systems will contaminate

* To whom correspondence should be addressed. E-mail: guangshe@fjirsm.ac.cn.

(1) Huang, M. H.; Mao, S.; Feick, H.; Yan, H. Q.; Wu, Y. Y.; Kind, H.; Weber, E.; Russo, R.; Yang, P. D. *Science* **2001**, *292*, 1897.
(2) Pan, Z. W.; Dai, Z. R.; Wang, Z. L. *Science* **2001**, *291*, 1947.
(3) Yang, J. L.; An, S. J.; Park, W. I.; Yi, G. C.; Choi, W. *Adv. Mater.* **2004**, *16*, 1661.
(4) (a) Guo, L.; Ji, Y. L.; Xu, H. B.; Simon, P.; Wu, Z. Y. *J. Am. Chem. Soc.* **2002**, *124*, 14864. (b) Gao, P. X.; Ding, Y.; Mai, W. J.; Hughes, W. L.; Lao, C. S.; Wang, Z. L. *Science* **2005**, *309*, 1700.
(5) Yu, H. D.; Zhang, Z. P.; Han, M. Y.; Hao, X. T.; Zhu, F. R. *J. Am. Chem. Soc.* **2005**, *127*, 2378.
(6) Wang, Z. L. *Mater. Today* **2004**, *7*, 26.
(7) Yan, H. Q.; He, R. R.; Johnson, J.; Law, M.; Saykally, R. J.; Yang, P. D. *J. Am. Chem. Soc.* **2003**, *125*, 4728.
(8) (a) Jiang, C. L.; Zhang, W. Q.; Zou, G. F.; Yu, W. C.; Qian, Y. T. *J. Phys. Chem. B* **2005**, *109*, 1361. (b) Xie, R. G.; Li, D. S.; Zhang, H.; Yang, D. R.; Jiang, M. H.; Sekiguchi, T.; Liu, B. D.; Bando, Y. S. *J. Phys. Chem. B* **2006**, *110*, 19147.
(9) Li, L. P.; Qiu, X. Q.; Li, G. S. *Appl. Phys. Lett.* **2005**, *87*, 124101.
(10) (a) Spanhel, L.; Anderson, M. A. *J. Am. Chem. Soc.* **1991**, *113*, 2826. (b) Xu, H. Y.; Wang, H.; Zhang, Y. C.; Wang, S.; Zhu, M. K.; Yan, H. *Cryst. Res. Technol.* **2003**, *38*, 429. (c) Wang, B. G.; Shi, E. W.; Zhong, W. Z. *Cryst. Res. Technol.* **1998**, *33*, 937.
(11) (a) Miguel, M.; Myrtil, L. K.; André, M.; Bruno, C. *Angew Chem. Int. Ed.* **2003**, *42*, 5321. (b) Zhang, Z. P.; Yu, H. D.; Shao, X. Q.; Han, M. Y. *Chem.—Eur. J.* **2005**, *11*, 3149.
(12) (a) Tian, Z. R.; Voigt, J. A.; Liu, J.; Mckenzie, B.; Mcdermott, M. J. *J. Am. Chem. Soc.* **2002**, *124*, 12954. (b) Demir, M. M.; Munoz-Espi, R.; Lieberwirth, I.; Wegner, G. *J. Mater. Chem.* **2006**, *16*, 2940.

10.1021/ic702348c CCC: $40.75
Published on Web 04/16/2008

the sample surfaces and moreover increase the difficulty in achieving sample uniformity, since these surfactants or polymers are generally strongly bonded to ZnO surfaces. To remove these absorbed species, high-temperature treatments have to take effect, which may in turn alter the morphology and put uncertain impacts on the physical properties. Moreover, surfactants and polymers also complicate the formation processes. Though the building processes of ZnO architectures have been widely described by various methods,[15] little is known about the chemical reactions that involve the solvents, surfactants, or polymers. From the chemical thermodynamics and kinetics viewpoints, these reactions might play a key role in forming ZnO architectures. As a consequence, it is of great value to find low-temperature synthetic techniques to prepare ZnO of special morphologies without involving any bases, surfactants, or polymers, which can help to get into the possible reaction mechanism for morphological and property tailoring.

In this work, we developed a simple solvothermal method to prepare a unique ZnO twin-cone structure without involving any bases, surfactants, or polymers during the formation reactions. By analyzing the compositions of the residual solutions, we discussed the formation mechanisms of ZnO twin-cones. The photoluminescence properties and the catalytic roles toward ammonium perchlorate decomposition were also explored.

2. Experimental Section

2.1. Sample Preparation. Chemicals of zinc nitrate hexahydrate ($Zn(NO_3)_2 \cdot 6H_2O$) and absolute ethanol (C_2H_5OH) were analytical grade and utilized without further purification. All samples were prepared according to the following experimental procedure: 5.9498 g (0.02 mol) $Zn(NO_3)_2 \cdot 6H_2O$ was completely dissolved into 150 mL C_2H_5OH with stirring at room temperature to form a transparent solution. This batch solution was transferred equally into the 6 Teflon-lined stainless steel autoclaves with a filling capacity of 30 mL. To study the temperature dependence of the evolution of the final products, these autoclaves were allowed to react at temperature from 120 to 160 °C for 4–6 h. To study the reaction time dependence of the evolution of the final products, these autoclaves were kept at 160 °C for specific periods of time. After cooling to room temperature, white solid products were collected by filtrating and washed with distilled water for several times, and dried in air at ambient condition.

2.2. Sample Characterization. The morphologies of the samples were investigated by a field-emission scanning electron microscopy (SEM) using a JEOL JSM-6700 apparatus and transmission electron microscopy (TEM) on a JEOL JEM 2010 instrument under an acceleration voltage of 200 kV. Phase compositions of the samples were characterized by powder X-ray diffraction (XRD) at room temperature on a Rigaku D/MAX25000 diffractometer with a copper target. The lattice parameters of the samples were obtained by structural refinement using Retica Rietveld program. Nickel powders were used as the internal standard for peak position calibrations.

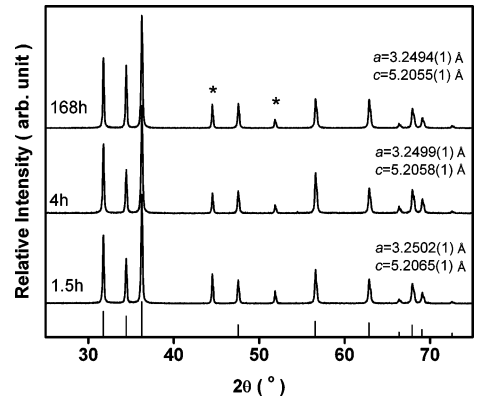

Figure 1. XRD patterns of the samples prepared at 160 °C for given periods of time. The * symbol denotes the diffraction peaks of internal standard Ni. Vertical bars below the patterns represent the standard diffraction data for wurtzite ZnO from the JCPDS file (No. 36-1451).

Infrared spectra of the residual solutions after formation reactions were measured using a Perkin-Elmer IR spectrophotometer (Spectrum One) at a resolution of 4 cm^{-1}. UV–visible absorption spectra of the residual solutions after formation reactions were recorded on UV–vis spectrometer Lambda 35 in the wavelength range from 200 to 700 nm. The chemical species in the intermediate residual solutions during the reactions were also analyzed using an ion trap mass spectrometry (DECAX-30000 LCQ Deca XP). The carbon content from the chemical species bonded on the sample surfaces were quantitatively determined by a combustion analytic method.

Photoluminescence spectra of the as-prepared samples were collected using He−Cd laser with the wavelength of 325 nm as the excitation source. All as-prepared samples were also studied as an additive in the thermal decomposition of 180 μm ammonium chlorite (AP) using the STA449C thermal analyzer at a heating rate of 20 °C min^{-1} in N_2 atmosphere over the range of 30–500 °C. AP and ZnO twin-cones were mixed at a mass ratio of 98:2 to prepare the target samples for thermal decomposition analyses. A total sample mass of 3.0 mg was used for all runs.

3. Results and Discussion

Figure 1 shows XRD patterns of the products prepared at 160 °C for given periods of time. The standard diffraction data for ZnO are also shown for comparison. It is seen that all diffraction peaks of the products are in good agreement with the standard data for ZnO (JCPDS 36-1451). No impurity peaks were detected. These results indicated that the products crystallized in a pure hexagonal wurtzite structure. The narrow and intense diffraction peaks indicated the presence of relatively large particle sizes which is confirmed by our SEM observation (Figure 4). The lattice parameters of the samples were given in Figure 1. It is seen that with increasing the reaction time from 1.5 to 168 h, the lattice parameters, *a* and *c*, decreased slightly from 3.2502(1) and 5.2065(1) to 3.2492(1) and 5.2055(1) Å, respectively.

(13) (a) Liu, B.; Yu, S. H.; Zhang, F.; Li, L. J.; Zhang, Q.; Ren, L.; Jiang, K. *J. Phys. Chem. B* **2004**, *108*, 4338. (b) Gao, S. Y.; Zhang, H. J.; Wang, X. M.; Deng, R. P.; Sun, D. H.; Zheng, G. L. *J. Phys. Chem. B* **2006**, *110*, 15847.

(14) (a) Taubert, A.; Kubel, C.; Martin, D. C. *J. Phys. Chem. B* **2003**, *107*, 2660. (b) Wang, Y. S.; Thomas, P. J.; O'Brien, P. *J. Phys. Chem. B* **2006**, *110*, 4099. (c) Tong, Y. H.; Liu, Y. C.; Dong, L.; Zhao, D. X.; Zhang, J. Y.; Lu, Y. M.; Shen, D. Z.; Fan, X. W. *J. Phys. Chem. B* **2006**, *110*, 20263. (d) Choi, S. H.; Kim, E. G.; Park, J.; An, K.; Lee, N.; Kim, S. C.; Hyeon, T. *J. Phys. Chem. B* **2005**, *109*, 14792. (e) Gao, X. P.; Zheng, Z. F.; Zhu, H. Y.; Pan, G. L.; Bao, J. L.; Wu, F.; Song, D. Y. *Chem. Commun.* **2004**, 1428. (f) Kuo, C. L.; Kuo, T. J.; Huang, M. H. *J. Phys. Chem. B* **2005**, *109*, 20115. (g) Krishna, K. S.; Mansoori, U.; Selvi, N. R.; Eswaramoorthy, M. *Angew. Chem., Int. Ed.* **2007**, *46*, 5962.

(15) (a) Lao, J. Y.; Wen, J. G.; Ren, Z. F. *Nano lett.* **2002**, *2*, 1287. (b) Zhang, T. R.; Dong, W. J.; Keeter-Brewer, M.; Konar, S.; Njabon, R. N.; Tian, Z. R. *J. Am. Chem. Soc.* **2006**, *128*, 10960.

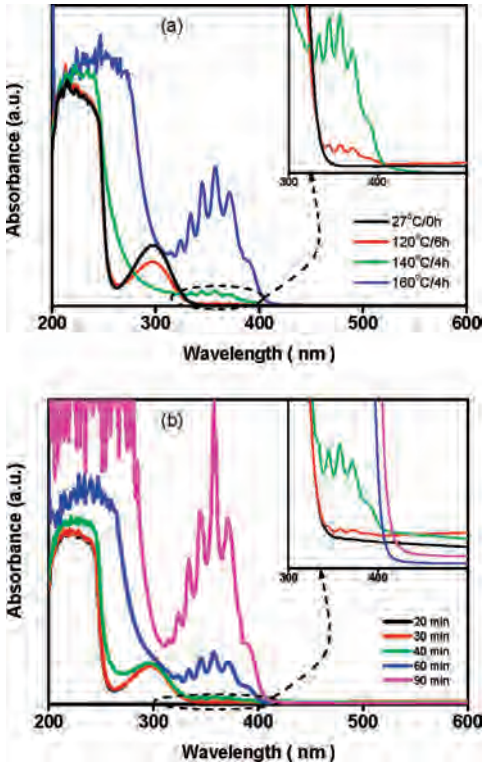

Figure 2. UV–visible spectra of (a) prereaction solution (27 °C, 0 h) and the residual solutions after formation reaction at given temperatures and (b) the residual solutions after reactions at a fixed temperature of 160 °C for given periods of time. All absorption spectra were recorded by taking ethanol as the reference.

Comparatively, the lattice parameter, *c*-axis, increases by 0.003 or 0.01 Å when the diameter of ZnO nanorods increased from 9 to 25 nm[9] or when ZnO film was annealed under vacuum in 300 °C for 1 h.[16] It is thus clear that the relative changes in lattice parameters for the present samples are obviously smaller than those contributed by particle size or oxygen content. Furthermore, IR spectra of the as-prepared samples indicated the presence of surface hydration layers and traces of residual organic carbon species (S1). The amounts of the carbon content was determined to be 1.2 wt % by a combustion analysis method.

Previously, the special morphologies of nanoscale inorganic compounds are stabilized by strong bases or templates such as surfactants or polymers.[10–14] For the present work, as indicated by SEM photos in Figure 4, the products were in a twin-cone shape. Since no bases were involved in the formation reactions, what, then, is the formation mechanism of ZnO twin-cones? We explored the reaction mechanism by studying the UV–visible, infrared absorption, and ion trap mass spectra of the residual solutions collected at different stages of the formation reactions. Figure 2 shows the UV–visible absorption spectra of the residual solutions. For the prereaction solution ($T = 27$ °C and $t = 0$ h), one broad absorption peak was observed at about 300 nm (Figure 2a), which is assigned to the excitation of a lone-pair, nonbonding electron (*n* orbital) of oxygen into an antibonding π orbital (π^* orbital) of the nitrate species (–O–NO_2).[17] After formation reaction at $T = 120$ °C for $t = 6$ h, the residual solution exhibited a similar broad absorption band to that of the prereaction solution except for a set of very weak peaks in the range from 320 to 400 nm (inset of Figure 2a). When the formation reactions were performed at 140 °C for 4 h, the broad absorption associated with the –O–NO_2 bond was hardly seen, while the set of peaks in the range from 320 to 400 nm became strong in intensity. Further increasing the reaction temperature up to 160 °C significantly intensified the fine structure of the set of peaks in the range from 320 to 400 nm. In addition to the reaction temperature, reaction time has also imposed an important influence on the evolution of the UV–visible absorption spectra of the residual solutions. Figure 2b illustrates the UV–visible spectra of the residual solutions after formation reaction at 160 °C for given periods of time. When the reaction time was shorter than 20 min, only one broad absorption peak for nitrate species was observed at about 300 nm, almost the same as that observed for the prereaction solution. When the reaction time was prolonged for 30 min, the set of very weak peaks in the range of 320 to 400 nm appeared (inset of Figure 2b). The broad absorption at about 300 nm for –O–NO_2 became weaker with prolonging the reaction time to 60 min, while the set of the fine structure in the range from 320 to 400 nm became stronger. When the reaction time was increased to 90 min, the fine structure of the absorption in the range of 320 to 400 nm became outmost pronounced, while the broad absorption for –O–NO_2 disappeared, which indicates the complete decomposition of the nitrate species. This conclusion is also confirmed by our infrared spectra (Figure 3) and ion trap mass spectral analysis (S2).

In order to explore the origin of the set of peaks in the range of 320 to 400 nm, a parallel experiment was performed in which zinc nitrate was replaced by nitric acid, while the other preparation parameters were kept the same. It is seen that the residual solution after reaction of ethanol with nitric acid or zinc nitrate at 160 °C for 4 h gave the similar fine structure in the UV–visible absorption spectrum (S3). It is well-known that when the organic molecules are exposed to light irradiation, six electronic transitions among σ, π, n, σ^*, and π^* may occur. The σ and σ^* levels in organic molecules are far apart in energy. Thus, the electronic transitions between σ and σ^* do not give rise to any absorptions above 250 nm. For example, ethanol, an organic molecule with only sigma type orbital, is transparent in the range from 200 nm to the visible wavelength. According to the assignments in literature,[18] the fine structures observed in the range of 320 to 400 nm in Figure 2 should be associated with the presence of certain new organic species that were derived from the reactions between ethanol and nitrate species. This conclusion could be understood by considering the redox potentials. It is well documented that the electrode potential of ethanol related to acetaldehyde is around −0.197 V at standard conditions, while that of nitrate is about 0.4 V ($\varphi_{NO_2^-}/NO_3^-$

(16) Cui, M. L.; Wu, X. M.; Zhuge, L. J.; Meng, Y. D. *Vacuum* **2007**, *81*, 899.

(17) Smith, G. P.; Boston, C. R. *J. Chem. Phys.* **1960**, *34*, 1396.

(18) Khibaum, G.; Tyutyulkov, N.; Ivanova, M. *Theor. Experiment. Chem.* **1973**, *6*, 484.

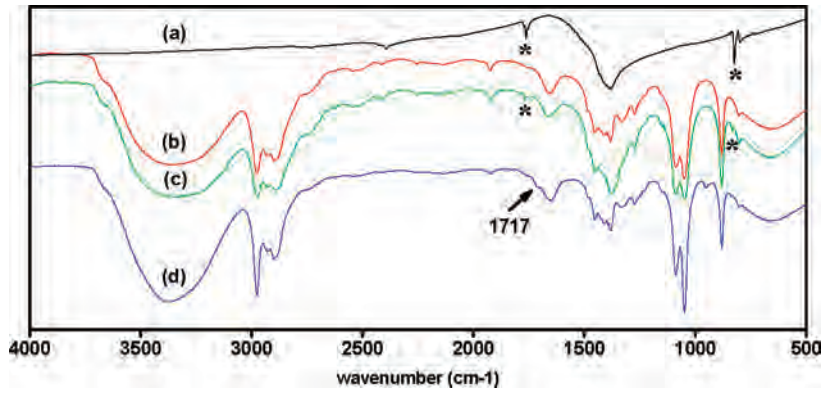

Figure 3. IR spectra of (a) nitrate, (b) ethanol, (c) prereaction solution, and (d) residual solution after formation reactions at 160 °C for 4 h. The * symbols represent the characteristic absorptions of nitrate species.[21]

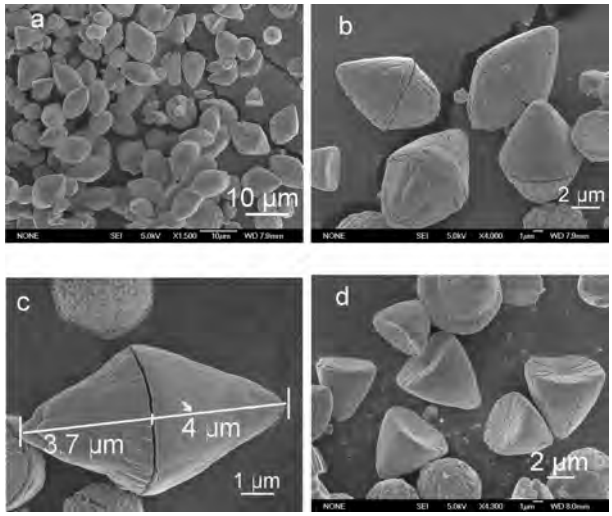

Figure 4. SEM images of the as-prepared ZnO sample prepared at 160 °C for 4 h: (a) low-magnification, (b) high-magnification, (c) enlarged SEM images of individual twin-cone, and (d) SEM images of the single ZnO cones.

$= 0.421V$, $\varphi_{NH_4^+/NO_3^-} = 0.36V$). That is, nitrate species could possess enough potential to oxidize ethanol.[19] These experimental observations are of fundamental significance since the formation of ZnO twin-cones is based on the redox reaction between ethanol and nitrate, which does not need any bases, surfactants, or polymers.

The creation of new chemical species from the formation reactions was also conformed by IR spectral analysis of the residual solutions after reactions at 160 °C for 4 h. For comparison, IR absorption spectra of the prereaction solution, ethanol, and nitrate solutions were also presented in Figure 3. It is seen that the IR spectrum of the prereaction solution is only a simple mixing of the absorptions from nitrate and ethanol species. When the formation reaction was ended, the absorption peaks associated with nitrate species disappeared, which is consistent with our analysis of UV–visible absorption spectrum. Moreover, a new absorption was observed at 1717.2 cm^{-1}, which can be attributed to the typical absorption of C=O bonds.[20]

To understand the origin of this C=O bond and the possible derivatives, ion trap mass spectra of the residual solution were measured. Four signals with $m/z = 69.5$, 114, 115.1, and 115.8 were observed (S2). Signals of $m/z = 69.5$ and 114 are associated with the $CH_3CH{=}CHCHO$ and $CH_3CH{=}CHCOOC_2H_5$, respectively, while those of $m/z = 115.1$ and 115.8 are attributed to the isotopic species of $CH_3CH{=}CHCOOC_2H_5$. No signals were detected at $m/z = 62$, which indicates the absence of nitrate species after formation reactions. Therefore, the formation reactions of ZnO twin-corns could proceed through the following routes:

$$4CH_3CH_2OH + NO_3^- \rightarrow 4CH_3CHO + NH_3\uparrow + OH^- + 2H_2O \quad (1)$$

$$Zn^{2+} + 2OH^- \rightarrow ZnO + H_2O \quad (2)$$

$$2CH_3CHO \xrightarrow{OH^-} CH_3CH(OH) - CH_2CHO(\text{aldol condensation}) \quad (2.1)$$

$$CH_3CH(OH) - CH_2CHO \xrightarrow{\text{dehydration}} CH_3CH{=}CHCHO + H_2O \quad (m/z = 70) \quad (3)$$

$$CH_3CH{=}CHCHO \xrightarrow{[O]} CH_3CH{=}CHCOOH \quad (4)$$

$$CH_3CH{=}CHCOOH + CH_3CH_2OH \rightarrow CH_3CH{=}CHCOOC_2H_5 \quad (m/z = 114) \quad (5)$$

Therefore, the functional groups of C=O in the residual solution as detected by IR spectra could be associated with the newly formed organic species which explains the set of weak absorptions in UV–visible spectra in the range of 320–400 nm.

The morphologies of the as-prepared samples were observed by SEM. Figure 4a and b show the SEM images of the samples that were obtained at 160 °C for 4 h. It is clear that the majority of ZnO particles were distributed in the shape of twin-cones. Prolonging the period of reaction time up to 148 h did not show apparent changes in the morphology. Magnified SEM images of the samples (Figure 4c) indicated the presence of a well-resolved slit in the twin-cone structure. Though both sides of the ZnO twin-cones

(19) (a) Fanning, J. C. *Coord. Chem. Rev.* **2000**, *199*, 159. (b) Hutson, A. C.; Sen, A. *J. Am. Chem. Soc.* **1994**, *116*, 4527.
(20) Hong, R. Y.; Pan, T. T.; Qian, J. Z.; Li, H. Z. *Chem. Eng. J.* **2006**, *119*, 71.

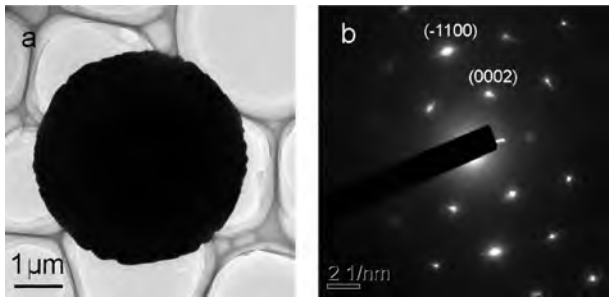

Figure 5. (a) TEM image for the round base and (b) selected electron diffraction pattern for an individual cone.

are slightly different (Figure 4c), the bottoms of both twin-cones are compatible each other with a diameter of 4 μm, indicating a special growth process. Figure 4d gives the SEM images of the single ZnO cones that were selected from the majority twin-cone products. An individual cone is seen to show a circular cross section of round-bottom as indicated by TEM image (Figure 5a). Selected electron diffraction pattern indicates that these individual cones possessed a single-crystal hexagonal structure, as characterized by different sets of lattice plane, (0002) for {0001} and (−1100) for $\{1\bar{1}00\}$ (Figure 5b). Surprisingly, the intensities of diffraction spots are not identical. Consequently, the round base of cones is not consisted by only one crystal plane because of the nonflat base (Figure 4d). In comparison with the hexagonal shaped ZnO cones previously reported in literature,[22] our ZnO twin-cones are distinct for the absence of any obvious hexagonal edges and corner. Twin-structures are not new and have been previously reported in Si, CuO, and ZnS;[23,24] nevertheless, the twin-cones discovered in this work are never observed in all ZnO family. In addition, the tiny boundary between ZnO twin-cones is fundamentally important which may block the motion of dislocation and therefore have significant impacts on the electronic and optical properties[25] for many technological applications.

The more exciting observation is the evolution of ZnO single crystal structures toward the formation of twin-cones. Figure 6 shows the scheme of morphological evolution of undeveloped ZnO along with the corresponding SEM images. As mentioned above, the formation of ZnO in present condition is strongly dependent on the reaction temperature and time. In the early growth stage of ZnO twin-cones, some amounts of ZnO nanoparticles are generated (S4) following the reaction path in eq 2, which could serve as the seeds or nucleation centers to form larger ZnO particles via Ostwald

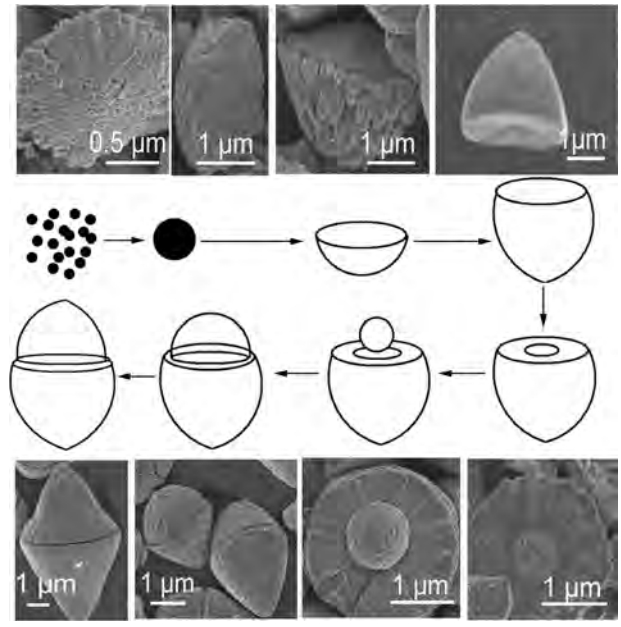

Figure 6. Morphological evolution of ZnO twin-cones.

ripening mechanism. TEM observations for the edge of cones (S5) also prove this assumption. The ZnO nanoparticles formed in the early growth stage are poorly crystallized, aggregated, and undergo a subsequent development toward the formation of single crystals. Consequently, single ZnO cones were structurally and energetically favorable to form under the present preparation condition. It is known that ZnO has both polar and nonpolar crystal surfaces, in which the former ones have higher surface energies for growth velocity than the later ones. Therefore, the [0001] direction (*c*-axis) has a highest growth rate.[26] The surfaces with a faster growth rate continually decrease their area, while the surfaces with slower growth rate gradually dominate the morphology of the resulting crystals. Therefore, most of the ZnO particles with special shapes such as hexagonal cone-shaped, pyramid, and tetrapods are grown along [0001] direction. The cones prepared in this work might have the same growing direction in which the cone bottoms served as the growth centers of the other cone. As evidenced in Figure 6, there is a small subunit in the middle of cone bottom, which grew larger and developed to yield the twin-cone structures. Since no templates were used during the formation reaction, the products of twin-cones are solid structure rather than the hollow structures as reported for many kinds of oxides.[27] As revealed by UV–visible spectra of the residual solution after reactions at different temperatures for given periods of time (Figure 2b), the reaction rate of eq 1 is slow. Since the Ostwald ripening process is related to the extremely low reaction rate,[28] it is likely that the small ZnO particles initially formed in eq 2 can have enough time to aggregate and

(21) Nyquist, R. A.; Kagel, R. O. *Infrared Spectra of Inorganic Compounds*; Academic Press: New York, 1971; p 134.
(22) (a) Ren, X. L.; Han, D.; Chen, D.; Tang, F. Q. *Mater. Res. Bull.* **2007**, *42*, 807. (b) Joo, J.; Kwon, S. G.; Yu, J. H.; Hyeon, T. *Adv. Mater.* **2005**, *17*, 1873. (c) Han, X. H.; Wang, G. Z.; Jie, J. S.; Choy, W. C. H.; Luo, Y.; Yuk, T. I.; Hou, J. G. *J. Phys. Chem. B* **2005**, *109*, 2733. (d) Wang, H. H.; Xie, C. S.; Zeng, D. W. *J. Cryst. Growth* **2005**, *277*, 372.
(23) (a) Carim, A. H.; Lew, K. K.; Redwing, J. M. *Adv. Mater.* **2001**, *13*, 1489. (b) Jiang, X. C.; Herricks, T.; Xia, Y. N. *Nano Lett.* **2002**, *2*, 1333. (c) Meng, X. M.; Jiang, Y.; Liu, J.; Lee, C. S.; Bello, I.; Lee, S. T. *Appl. Phys. Lett.* **2003**, *83*, 2244.
(24) Tang, J.; Cui, X. Q.; Liu, Y.; Yang, X. R. *J. Phys. Chem. B* **2005**, *109*, 22244.
(25) Zhang, Z. H.; Liu, H. H.; Jian, J. K.; Zou, K.; Duan, X. F. *Appl. Phys. Lett.* **2006**, *88*, 193101.
(26) Li, W. J.; Shi, E. W.; Zhong, W. Z.; Yin, Z. W. *J. Cryst. Growth* **1999**, *203*, 186.
(27) (a) Mo, M.; Yu, J. C.; Zhang, L. Z.; Li, S. K. A. *Adv. Mater.* **2005**, *17*, 756. (b) Zhan, S. H.; Chen, D. R.; Jiao, X. L.; Tao, C. H. *J. Phys. Chem. B* **2006**, *110*, 11199. (c) Yu, H. G.; Yu, J. G.; Liu, S. W.; Mann, S. *Chem. Mater.* **2007**, *19*, 4327.
(28) Adschiri, T.; Hakuta, Y.; Sue, K.; Arai, K *J. Nanoparticle Res.* **2001**, *3*, 227.

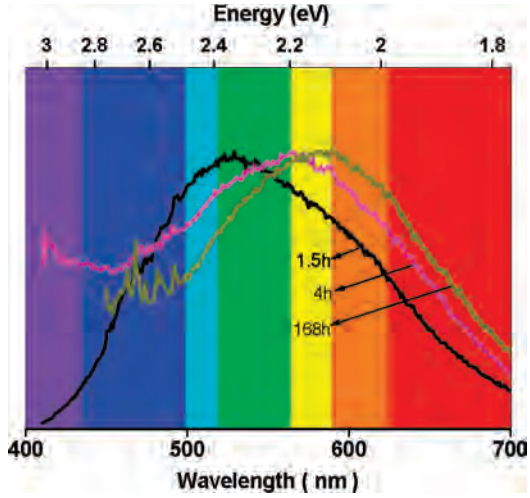

Figure 7. Photoluminescence spectra of ZnO twin-cones prepared at 160 °C for given periods of time.

coarsen to ZnO twin-cones. It is also noted that, as for TiO_2 and many other oxide materials,[29] water content determines the initial species formed during the hydrolysis and therefore strongly impacts the resultant phase produced. For the present work, there exist some amounts of water molecules originated from the starting zinc nitrate hexahydrate and from the reaction eqs 1−3 as well, while the impact of water could be negligible since the water concentration is extremely low at 0.08 mol/100 mL in the starting solution. Instead, when plenty of water molecules were involved in the formation reactions such as at a water/ethanol volume ratio of 1/15, a novel morphology of ZnO twin-prisms was obtained (S6).

To further characterize the defect feature of these twin-cones ZnO, photoluminescence spectra with an excitation wavelength of 375 nm were measured. As shown in Figure 7, all ZnO twin-cones displayed a broad asymmetric emission with the peak position varying with the reaction conditions. For instance, ZnO cones obtained after reaction at 160 °C for 1.5 h showed an emission centered around 527 nm, which is identified as a green emission band. When the reaction time was prolonged to 4 h, the emission band shifted to 565 nm in the yellow spectral range. Further prolonging the reaction time to 168 h, the emission peak shifted to about 580 nm, near to the orange spectral range. This observation is surprising since ZnO is a wide band gap semiconductor (3.4 eV) that usually shows a near band-edge emission at 380nm.[29] Because of the existence of intrinsic defects, photoluminescence at visible region is usually observed for both bulk and nanoparticles of ZnO.[8,13] The nature of green emission remained controversial for decades. In the early studies about the ZnO single crystals, it is attributed to the impurities such as Cu. But, much evidence presented recently for nanosize ZnO suggests that it should be associated with the donor levels of oxygen vacancy (V_o),[30] while the yellow or longer wavelength emissions are ascribed to contribution of interstitial oxygen (O_i).[31] The observation of green emission for twin-cones ZnO obtained at short reaction time indicates that oxygen vacancies are formed at the beginning of crystallization of ZnO particles. With increasing the reaction time, the emission shifted toward longer wavelength, indicating a decrease of V_o concentration and the introduction of O_i. The variation of defect species vs reaction time might be related to the formation energy of these intrinsic defects. First-principles calculation[32] has revealed that oxygen vacancies V_o of ZnO have the lowest formation energy under zinc-rich conditions. However, under oxygen-rich conditions, either oxygen interstitials O_i or doubly negatively charged zinc vacancy (V_{Zn}'') could become the dominant defect for bulk ZnO as is determined by the position of Fermi level. For the present work, ZnO twin-cones were formed by a solvothermal condition, an oxygen-poor system, which might favor to form the oxygen vacancies as indicated by the observed green emission. Comparatively, the nanoseeds prepared at room temperature in air, an oxygen-rich condition, exhibited an emission centered at 603 nm.[9] The very broad asymmetric emission may also be contributed by V_o- and the O_i-related defect as well. Prolonging the reaction time resulted in an increase in the concentration of O_i-related defects. Therefore, at oxygen-poor conditions, O_i-related defects should be stable kinetically. The slight decrease of lattice parameters observed with reaction time might also reflect the relative variation of defect concentrations.

ZnO twin-cones were explored as an additive to the thermal decomposition of ammonium perchlorate (AP), the key component of composite solid propellants. The performance of ZnO twin cones in the thermal decomposition of AP was investigated by TG-DSC measurements. From the TG curves (S7), it is seen that in the temperature range from room temperature to 500 °C, only one mass loss was observed for both pure AP and mixture of AP with ZnO cones prepared at 160 °C for 4 h. The addition of ZnO cones dramatically decreased the AP decomposition temperature, consistent with our DSC measurements. Figure 8 shows the DSC curves of both pure AP and the mixture of AP with ZnO cones at a 2% mass basis. Only two thermal signals were observed for mixture of AP with ZnO cones, which compares to the three obvious peaks for pure AP. The first endothermic peak at 240 °C is due to the crystal transformation of AP from orthorhombic to cubic phase, while the second exothermic peaks occurred at temperatures above 300 °C are attributed to the AP decomposition. The thermal decomposition of pure AP, depending on the quality of crystals, usually undergoes two or more steps. From Figure 8, it is seen that, for pure AP, there are two obvious exothermic peaks centered at about 338 and 442 °C, which correspond to the low-temperature decomposition (LTD) and

(29) Ardizzone, S.; Bianchi, C. L.; Cappelletti, G.; Gialanella, S.; Pirola, C.; Ragaini, V. *J. Phys. Chem. C.* **2007**, *111*, 13222, and references therein.
(30) Liu, B.; Zeng, H. C. *J. Am. Chem. Soc.* **2004**, *126*, 16744.
(31) (a) Vanheusden, K.; Warren, W. L.; Seager, C. H.; Tallant, D. R.; Voigt, J. A.; Gnade, B. E. *J. Appl. Phys.* **1996**, *79*, 7983. (b) Osaga, K.; Sakurai, K.; Fujita, S.; Fujita, S.; Matsushige, K. *J. Cryst. Growth* **2000**, *214*, 312.
(32) (a) Greene, L. E.; Law, M.; Goldberger, J.; Kim, F.; Johnson, J. C.; Zhang, Y.; Saykally, R. J.; Yang, P. *Angew. Chem., Int. Ed.* **2003**, *42*, 3031. (b) Li, D.; Leung, Y. H.; Djurišić, A. B.; Liu, Z. T.; Xie, M. H.; Shi, S. L.; Xu, S. J.; Chan, W. K. *Appl. Phys. Lett.* **2004**, *85*, 1601.

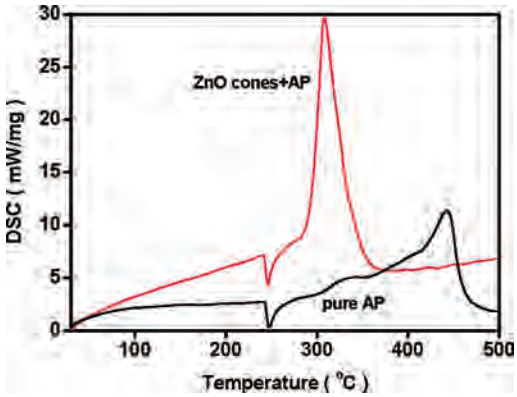

Figure 8. DSC curves of pure AP and the mixture of AP with ZnO twin-cones that were prepared at 160 °C for 4 h. The mass percentage of ZnO to AP in the mixture is fixed at 2%.

high-temperature decomposition (HTD), respectively. The low-temperature decomposition has been proposed to be a heterogeneous process which includes a proton transfer in the AP subsurface to yield NH_3 and $HClO_4$, the adsorption of NH_3 and $HClO_4$ in the porous structure, and finally the decomposition of $HClO_4$ and reaction with NH_3.[33] Alternatively, the high-temperature exothermic process is due to the oxidation of NH_3 by $HClO_4$ in the close sample pans. The total process can be expressed as follows:[34,35]

$$NH_4ClO_4 \rightleftharpoons NH_3{-}H{-}ClO_4 \rightleftharpoons NH_3{-}HClO_4 \rightleftharpoons NH_{3(a)} + HClO_{4(a)} \quad \text{(LTD)} \quad (6)$$

$$NH_{3(a)} + HClO_{4(a)} \rightleftharpoons NH_{3(g)} + HClO_{4(g)} \quad \text{(HTD)} \quad (7)$$

A significant difference for AP decomposition with and without additive ZnO twin-cones is the disappearance of high-temperature process, which should be associated with the concentration reduction of $NH_{3(a)}$ and $HClO_{4(a)}$. On the one hand, V_o-related defects are usually formed in the poor-oxygen condition,[33,36] which may reduce the concentration of NH_3 partially. Since nitrogen gas passes though the samples and produces a poor-oxygen condition during the whole DSC measurement, some of interstitial oxygen, O_i^x or lattice oxygen, O_o^x, might transform to V_o-related defects and release oxygen in terms of the following processes:

$$O_o^x \rightarrow V_o^x + \frac{1}{2}O_2(g) \quad (8)$$

$$O_i^x \rightarrow V_i^x + \frac{1}{2}O_2(g) \quad (9)$$

where the superscript "x" denotes the neutral species. The oxygen released in eqs 8 and 9 might react with NH_3 to decrease the concentration of $NH_{3(a)}$. On the other hand, the reaction of ZnO twin-cones with $HClO_4$ to form $Zn(ClO_4)_2$ and the decomposition of $Zn(ClO_4)_2$ to release O_2 and Cl_2 also occurred in the temperature range of LTD.[37] Therefore, AP decomposition was accelerated in the presence of ZnO twin cones. It is also found that AP mixed with ZnO twin-cones prepared at 160 °C for different periods of time exhibited almost the same thermal decomposition behaviors, most likely due to the undistinguished differences of defect species and their concentration in addition to the similar particle size. Finally, the influence of ZnO cones on the decomposition temperature and conversion rate of AP is much more prominent than TiO_2 nanoparticles, since for the latter case, as indicated in S8, the addition of TiO_2 nanoparticles did not suppress the HTD process but only slightly decreased the temperature of HTD as is reported by Seal et al.[34]

4. Conclusions

ZnO twin-cones were directly prepared from a mixed solution of zinc nitrate with ethanol. UV–visible and IR spectra for the residual solutions at different stages of the reactions indicated that nitrate species were reduced as the formation reaction goes. The low reaction rate in the Ostwald ripening process could be the main reason for the formation of ZnO twin-cones with a relatively large size. TEM and selected electron diffraction pattern indicated that the cones possessed a single-crystal hexagonal structure. ZnO twin-cones exhibited a defect-relevant photoluminescence. With prolonging the reaction time from 1.5 h to 7 days, the emission peak shifted from the green to yellow region, which is associated with the increased interstitial oxygen concentration and decreased oxygen vacancy concentration. These defect characteristics also enable ZnO twin-cones to show merits in promoting the thermal decomposition of ammonium perchlorate.

Acknowledgment. This work was financially supported by NSFC under the contract (No. 20773132, 20771101, and 20671092), National Basic Research Program of China (973 program, No. 2007CB613306), Directional program (No. KJCX-YW-M05, FJIRSM (SZD07004-3)), and a grant from the Hundreds Youth Talents Program of CAS (Li GS). We would also like to thank the reviewers for critical comments. We also appreciate the assistance of Lijuan Chen for data recording of the thermal decomposition of ammonium perchlorate with TiO_2 nanoparticle additives.

Supporting Information Available: IR spectrum of the as-prepared ZnO twin-cones, Ion trap mass spectrum of residual solution, TEM and HRTEM images of the edge of ZnO cones, and TGA curves of AP decomposition. This material is available free of charge via the Internet at http://pubs.acs.org.

IC702348C

(33) Erhart, P.; Klein, A.; Albe, K. *Phys. Rev. B* **2005**, *72*, 825213.
(34) Reid, D. L.; Russo, A. E.; Carro, R. V.; Stephens, M. A.; LePage, A. R.; Spalding, T. C.; Petersen, E. L.; Seal, S. *Nano lett.* **2007**, *7*, 2157.
(35) Boldyrev, V. V. *Thermochim. Acta* **2006**, *443*, 1.
(36) Borseth, T. M.; Svensson, B. G.; Kuznetsov, A. Y.; Klason, P.; Zhao, Q. X.; Willander, M. *Appl. Phys. Lett.* **2006**, *89*, 262112.
(37) Solymosi, F.; Gera, L. *J. Phys. Chem.* **1971**, *75*, 491.